PHOTOINDUCED GEOMETRICAL REARRANGEMENT OF LITHIUM DOPED ARGON MATRICES

REORDENAMIENTO GEOMÉTRICO FOTOINDUCIDO EN MATRICES DE ARGÓN DOPADAS CON LITIO

E. L. Rodríguez-Rodríguez, L. Uranga-Piña[†], A. Martínez-Mesa

Facultad de Física, Universidad de la Habana, San Lázaro y L, Vedado, Habana, Cuba. llinersy@fisica.uh.cu[†]
† corresponding author.

The energetics of Li(2p ← 2s) photoexcitation in low-temperature ($T = 4\ K$) argon matrices is investigated via molecular dynamics simulations. Absorption and emission lineshapes are computed at the effective temperature of 31 K, which mimics zero-point energy effects on crystal site oscillations. Interaction forces are derived from an approximation to the energy of the electronic states of the doped solid, based on first order perturbation theory. The absorption band exhibit a three-fold structure, as a consequence of dynamic Jahn-Teller effect, the splitting being in close correspondence with available experimental results for this system. The relationship between transition energies and the photoinduced configurational rearrangement of the solid is also addressed. Lattice reorganization is found to be sensitive to the shallow long-range tail of the interatomic potentials, pointing to the feasibility to employ many-body response of doped matrices upon photoexcitation as a tool to study the topology of the excited electronic states of alkali-rare gas systems.

Las propiedades energéticas de la fotoexcitación de átomos de litio, Li(2p ← 2s), en matrices de argón a bajas temperaturas ($T = 4\ K$), es investigada a través de simulaciones con dinámica molecular. Los espectros de absorción y emisión son calculados a la temperatura efectiva de 31 K, la cual reproduce los efectos de la energía de punto cero sobre las oscilaciones de la red. Las fuerzas de interacción se derivan a partir de una aproximación de la energía de los estados electrónicos del sólido dopado, basada en la teoría de perturbaciones de primer orden. La banda de absorción exhibe una estructura de tres picos, como consecuencia del efecto Jahn-Teller dinámico, cuyo desdoblamiento se corresponde con los resultados experimentales disponibles para este sistema. También se analiza la relación entre las energías de transición y el reordenamiento configuracional fotoinducido. Se encontró que la reorganización del cristal es sensible a las débiles contribuciones de largo alcance de los potenciales interatómicos, lo que indica la factibilidad de emplear la respuesta colectiva de las matrices dopadas a la fotoexcitación como herramienta para estudiar la topología de los estados electrónicos excitados de los sistemas metal alcalino-gas noble.

I. INTRODUCTION

Alkali-rare gas diatomic molecules constitute ideal model systems for the study of van der Waals (vdW) interactions. Owing to its relative simplicity, the ground and excited electronic states of these molecules are usual targets of electronic structure calculations, in order to assess the quality of modern *ab initio* and model potential calculation methods [1-16]. The experiments measuring the index of refraction of atomic matter waves passing through a dilute rare gas environment have also contributed to the renewed interest on the interaction between alkali metal atoms and rare gas atoms [17].

Alkali-rare gas diatomics usually exhibit very shallow potential energy curves in their ground electronic state, while excited states present much larger binding energies. From the experimental view point, accurate spectroscopic data may provide very valuable information about the bound part of the interatomic potential. Nevertheless, many interesting features, such as the marked oscillations of interaction potentials for several excited states, appear to be out of reach for spectroscopic studies in the gas phase. On the other hand, condensed phase observables are expected to be sensitive enough to the form of the potential energy curves, as has been shown for the excitation of the first Rydberg state of lithium atoms embedded in argon matrices [18].

Likewise, rare gas matrices are especially suited for studying molecular spectroscopy. Optical absorption of doped rare gas solids enables retrieving information from both the impurity and the surrounding medium [19]. Since only acoustic phonons up to 100 meV exist in the solid [20], the latter is transparent to ultraviolet electromagnetic radiation, thus allowing to investigate the electronic excitation of lithium atoms without matrix interference. Argon crystals posses additional advantages as hosts, namely a modest role played by quantum delocalization effects (compared to lighter rare

gas atoms like neon or helium), which makes it possible the molecular dynamics simulation of the solid, and a rather low polarizability (compared to krypton and xenon), which keeps impurity-rare gas interactions, as well as three-body forces, small.

The aim of this work is to investigate the absorption and emission spectra of lithium doped argon matrices, as well as the geometrical rearrangement of the solid taking place after the electronic (2p ← 2s) excitation of the impurity. The relationship between transition energies, the photoinduced rearrangement of argon atoms around the impurity and the alkali-rare gas interatomic potentials is also addressed.

The organization of the paper is the following. In Section II, we briefly describe the main features of LiAr interaction potentials for the ground and excited states, together with the methodology applied to obtain the corresponding potential energy surfaces and to carry out the molecular dynamics simulations. In Section III, the results are presented and discussed. Finally, in Section IV some conclusions are drawn.

II. METHODOLOGY

Interatomic pair interactions. In the present work, the interaction between lithium and argon atoms in the molecular λ = X, A and B electronic states was modelled through Morse functions

$$V_\lambda(r) = D_\lambda \left[e^{-2\alpha_\lambda \left\{ r - r_e^{(\lambda)} \right\}} - 2e^{-\alpha_\lambda \left\{ r - r_e^{(\lambda)} \right\}} \right], \tag{1}$$

with state-dependent well depth D_λ, equilibrium bond length $r_e^{(\lambda)}$ and anharmonicity parameter α_λ. The potential parameters D_λ and $r_e^{(\lambda)}$ were set equal to the values obtained in previous theoretical investigations employing the coupled cluster method [5]. The values of α_λ were obtained from the least-squares fitting of the spectroscopic properties reported in Ref. [5], specifically the harmonic $\left(\omega_e = (2D_\lambda \alpha_\lambda^2 / \mu_{LiAr})^{1/2} \right)$ and anharmonic $\left(\omega_e x_e = \hbar^2 \alpha_\lambda^2 / 2\mu_{LiAr} \right)$ frequencies. In these expressions, which follow from the analytical solution of the time-independent Schrödinger equation for the Morse potential (1), μ_{LiAr} represents the reduced mass of the diatomic molecule. The parameters of the interaction potentials, for the three electronic states considered, are summarized in Table I. In Figure 1, the corresponding potential energy curves are shown. It can be seen, that the LiAr interaction is almost purely repulsive in the ground electronic state.

Table I			
LiAr interaction parameters used in this work.			
λ	D_λ [cm^{-1}]	$r_e^{(\lambda)}$ [Å]	α_λ [Å^{-1}]
X	39.10	4.940	0.908
A	889.02	2.545	1.979
B	29.32	6.280	0.874

Excitation of the alkali atom to the Li(2p) state leads to two

molecular states of different symmetry, namely the A$^2\Pi$ state, characterized by a relatively large well depth ($D_A \approx 900\ cm^{-1}$), and the repulsive B$^2\Sigma^+$ state. As a result of the different orientations of the rare gas atoms placed along the crystal axes, with respect to the symmetry axis of the valence orbital of the alkali metal, the electronic transition is expected to induce a lattice reorganization exhibiting a marked anisotropy.
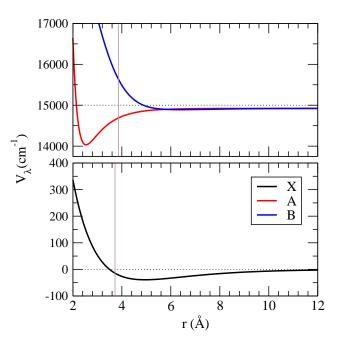

Figure 1. Potential energy curves corresponding to the X, A and B electronic states of the LiAr diatomic molecule. The vertical lines indicate the average nearest neighbor distance in argon crystals (bottom panel) and the average radius of the first shell around the impurity (upper panel), for the electronic ground state of the doped solid.

Potential energy surface. Owing to the closed shell electronic structure of the atoms, argon matrices interact only weakly with guest atoms or molecules. Since the atomic electron densities in the crystal are rather similar to the corresponding distributions in the gas phase, the potential energy surface of the system was represented as a superposition of interatomic pair potentials:

$$U_k(\mathbf{R}) = E_{LiAr}^{(k)}(\mathbf{R}) + \sum_{i<j}^{N} V_{ArAr}(|\mathbf{R}_i - \mathbf{R}_j|). \tag{2}$$

The vector $\mathbf{R} = \{\mathbf{r}, \mathbf{R}_1, ..., \mathbf{R}_N\}$ comprises the Cartesian coordinates of the impurity and the N argon atoms, respectively. The interaction V_{ArAr} between host atoms was modelled as a Lennard-Jones potential, whose parameters (ε = 83.9 cm^{-1}, σ = 3.405 Å) were taken from the literature [21].

In the ground state, there is only one potential energy curve which asymptotically correlates to the Li(2s)+Ar fragments, so the impurity-rare gas interaction $E_{LiAr}^{(0)}$ is given by the interatomic potential V_X. For the excited Li(2p) atom interacting with ground state argon atoms, the need to account for both Σ and Π diatomic interactions, enforces the use of a more elaborate approach. Therefore, the excited-state lithium-argon interaction is described within first-order perturbation

theory, following the method originally proposed Balling and Wright [22]. Within this approach, the interaction potential between the alkali atom and the rare-gas crystal is derived under the assumption that core electrons of the impurity remain unaffected by the matrix atoms. Hence, the Hamiltonian of the doped solid may be written in the atomic representation (which comprises the eigenstates of the valence electron of the lithium atom corresponding to the three different values of the magnetic quantum number: m = -1, 0, +1), where the matrix elements are summed over all diatomic Li-Ar contributions. The term $E^{(k)}_{LiAr}(\mathbf{R})$ (k = 1, 2, 3) is given by the kth-eigenvalue of the matrix

$$\mathbb{E}=\frac{1}{3}\sum_{i=1}^{N}\left\{\left[V_B(r_i)+2V_A(r_i)\right]\mathbb{I}+\frac{1}{2}\left[V_B(r_i)-V_A(r_i)\right]\mathbb{W}\right\}, \qquad (3)$$

$$det\,|\,\mathbb{E}-E\mathbb{I}\,|=0, \qquad (4)$$

where r_i denotes the lithium-argon interatomic distances $|\mathbf{r} - \mathbf{R}_i|$. Explicit expressions for the matrix elements of $\mathbb{W}$ can be found in Ref. [23].

Molecular Dynamics simulations. We performed 50 *ps* molecular dynamics (MD) simulations of lithium doped argon matrices, using the velocity Verlet algorithm with a time step of 1 *fs*. Prior to the computation of averages, the system is allowed to equilibrate during 10 *ps*, in order to ensure that the calculated absorption and emission spectra and structural indicators (e.g., radial distribution functions) correspond to the desired effective temperature T_{cl}= 31 *K*. The latter is the temperature at which the classical distribution of an oscillator, that collectively accounts for all crystal phonons, approaches the diagonal elements of the corresponding quantum density matrix [24] at the physical temperature T= 4 *K*. The system is composed by one lithium atom and 863 rare gas atoms, confined inside a simulation cell with linear dimensions of 31.82 *Å*, in order to reproduce the experimental density of the argon solid. The impurity occupies a substitutional site in the face centred cubic lattice. Periodic boundary conditions were imposed to minimize surface effects and to simulate an infinite solid.

The absorption and emission spectra are calculated according to the Franck-Condon principle, i.e., the electronic transition is assumed to take place instantaneously. If the matrix element of the transition dipole moment operator is assumed to be constant, then the probability of the system to hop from state k to k', as a consequence of the interaction with the external electromagnetic field, is given by

$$I_{kk'}(\omega)\propto\int\rho_k(\mathbf{R})\delta\big(U_{k'}(\mathbf{R})-U_k(\mathbf{R})-\hbar\omega\big)d^3\mathbf{R}, \qquad (5)$$

where ω is the frequency of the photon inducing the electronic transition. The equilibrium distribution $\rho_k(\mathbf{R})$, in the nuclear configuration space, is sampled by the MD trajectories evolving on the kth-potential energy surface. Therefore, the absorption spectra are constructed by collecting the energy differences between the ground and the excited state manifold $U_k(\mathbf{R})$, k = 1, 2, 3.

Based on previous semiclassical surface hopping studies on the dynamics of triplet states in argon matrices [25], the contributions to the emission spectra due to excited states, other than the lowest one $U_1(\mathbf{R})$, were neglected. This choice is justified by the fast depopulation of the two highest energy excited states, due to many crossings between the three potential energy surfaces. As a consequence, only the lowest excited surface is populated after a relaxation time of a few picoseconds.

III. RESULTS AND DISCUSSION

To the aim of analyzing the influence of the replacement of a rare gas atom by lithium, the radial distribution functions of solvent atoms around the impurity were calculated and compared to the corresponding pair distribution for the pure crystal. The latter was also generated via MD simulations. The results are shown in Figure 2. Since the potential energy surface can be decomposed in a sum of pair interactions, we included the relevant potential energy curves. Vertical dashed lines indicate the positions of the first two coordination shells around the atomic centre in the pure and the doped matrices. It can be seen, that the equilibrium positions of the nearest neighbor shell in the crystal (black dashed line) almost coincide with the bond length of the Ar-Ar interaction (3.8 Å). Upon substitution of one argon atom by the alkali metal, the rare gas atoms placed at nearest neighbor distance from the impurity centre experience a repulsive force. As indicated by the red dashed line, this first shell moves outwards by around 0.19 Å with respect to the pure solid. Further expansion of these atoms is prevented by the confinement imposed by the rest of the matrix.
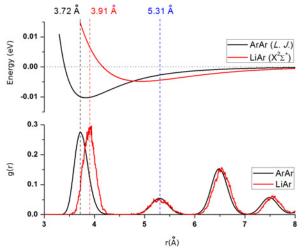

Figure 2. Upper panel: Potential energy curves corresponding to the interaction between Ar-Ar and Li-Ar pairs (in their electronic ground state). Lower panel: Radial distribution functions g(r) of argon atoms around an Ar (pure solid) or a Li (doped solid) atom. Vertical dashed lines indicate equilibrium radii of the first coordination shells from the atomic centre.

In Figure 2, it can also be noticed that the second neighbor shell is not affected by the presence of the impurity. Its average distance is essentially the same than for the pure solid (equal to the lattice constant, 5.3 Å). It follows from the Li-Ar and

16

the Ar-Ar potential energy curves, that the forces exerted on the rare gas atoms forming this shell atoms are very similar in both cases. Additionally, these atoms are not located on the crystallographic axis (110), defined by the lithium atom and its nearest neighbors, so no shifts are expected as a consequence of the change in the position of the radius of the first shell. The rare gas atoms in the first shell interact directly with those in the third and the fourth coordination shells, so their motion influence that of the latter. That causes the tiny displacement of the corresponding peaks depicted in Figure 2. It becomes apparent, that the insertion of the lithium atom at a lattice site cause only a small distortion of the surroundings, namely a small displacement of the nearest neighboring Ar atoms (the distance between these atoms and the impurity is about 5% larger than the corresponding separation in the pure crystal).

In Figure 3, we show the absorption and emission spectra corresponding to the transition between the electronic states 2s and 2p of the lithium atom embedded in an argon matrix. The absorption spectra clearly show the splitting of the triplet state of the alkali atom, due to the presence of matrix atoms, i.e., the perturbation originated by the atoms in the vicinity of the impurity removes the triple degeneracy, giving rise to three well defined absorption peaks centred at three different energies $E_1 = 1.837$ eV, $E_2 = 1.871$ eV and $E_3 = 1.903$ eV. These values nicely reproduce the Jahn-Teller splitting observed experimentally (Table 2), the deviations between experimental and theoretically computed values being of about 5%. Except for E_1, the remaining absorption energies are slightly blue shifted with respect to the transition energy for a free lithium atom (1.85 eV). On the other hand, the emission spectra exhibits a singlet structure, since the contributions from the transient populations of the excited states 2 and 3 has been neglected. As a consequence of the fast depopulation of these electronic states, we expect the emission from the lowest excited state 1, plotted in Figure 3, to be the only one present in spectra recorded in experiments carried out under equilibrium conditions. To our knowledge, there are not experimental reports on the luminescence of lithium doped argon matrices.
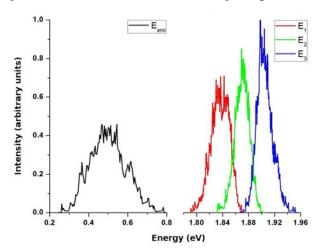

Figure 3. Absorption (blue, green and red curves) and emission (black curve) spectra of lithium doped argon matrices. The removing of the three-fold degeneracy of the 2p state of Li is clearly seen.

	Table II	
Energies of the maxima of absorption and emission spectra of Li doped Ar matrices. Experimental values were reported in Ref. [26]. All values are in eV.		
	MD	Expt. (Ref [26])
Absorption		
E_1	1.837	1.939
E_2	1.871	1.983
E_3	1.903	2.027
Emission		
E_{ems}	0.495	-
Stokes shift		
$E_1 - E_{ems}$	1.342	-

Since the large Stokes shift, $E_1 - E_{ems} = 1.342$ eV, is indicative of an extensive lattice rearrangement, we discuss the modification of the overall structure upon photoexcitation, in terms of the radial distribution functions. Since the optical excitation has local character, we focus on the pair correlation between the impurity and the nearby atoms, presented in Figure 4.
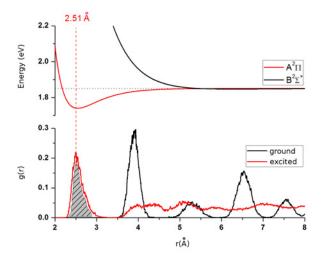

Figure 4. Upper panel: Potential energy curves corresponding to the A and B states of the LiAr diatom. Lower panel: Radial distribution functions $g(r)$ of argon atoms around the impurity centre in the ground (black) and excited (red) electronic states of the system. The vertical line corresponds to the average position of the 4 argon atoms which get attracted to the Li(2p) atom.

The transition of the lithium atom to the 2p state causes a reorganization of the surrounding media to a new equilibrium configuration, while the system explores simultaneously the three potential energy surfaces $U_1(\mathbf{R})$, $U_2(\mathbf{R})$ and $U_3(\mathbf{R})$. After a few picoseconds, all the population is transferred to the lowest-lying electronic state, $U_1(\mathbf{R})$, within the triplet manifold. The distribution of solvent atoms around the impurity dramatically changes as a consequence of this process. As it can be seen, some argon atoms are attracted closer to the impurity centre. The integration of the first peak of the excited state radial distribution function (grey area) yields that four particles move toward this new equilibrium position (2.51 $Å$). It is important to notice, that the 12 nearest neighbors of the lithium are placed at different angles with respect to the p orbital of the metal. Therefore, a subset of the first shell experience attractive forces coming from the A state contribution, while the rest evolves under the influence of an interaction potential which resembles

that of the B state. Then, the interaction of the atomic impurity with the rare gas environment, in the excited electronic state, is strongly anisotropic and a splitting of the former first shell takes place.

In Figure 4, it becomes striking that the geometrical rearrangement of the solid occurs for a region which is wider than the characteristic length scale of the excited state interaction potential. Then, it is chiefly governed by the displacement of the nearest neighbors of the impurity instead of being consequence of the direct interaction with the latter. In particular, a clear identification of solvation shells is no longer possible. This is caused not only by the reorganization of the rare gas media but due to the displacement of the lithium atom itself.

IV. CONCLUSIONS

We have presented a MD study of the absorption and emission spectra associated with the Li(2p ← 2s) electronic transition in argon atoms. Matrix effects cause energy shifts from -13 *meV* to 53 *meV* of the transition energy on absorption, compared to the gas phase, while the emission energies are strongly red shifted. The analysis of the radial distribution functions shows that a significant lattice reorganization takes place after the photoexcitation. In particular, a subset of four rare gas atoms get strongly attracted to the impurity, among those forming the nearest neighbor shell in the electronic ground state. The present study correlates the energetics of the optical absorption and the corresponding luminescence, as well as the leading aspects of lattice reorganization, to the main features of the LiAr potential energy surfaces, thereby confirming that matrix spectroscopy can reveal valuable information on alkali-rare gas interactions.

As an outlook, we aim to study the time evolution of the restructuring process, since a rich phenomenology is expected to arise as a consequence of the strongly anisotropic nature of excited state interactions and from the fact that the system evolves simultaneously on three potential energy surfaces. Because of the presence of many conical intersections, such investigation can not be carried out within the framework of purely classical mechanics, and molecular dynamics has to be complemented with algorithms (e.g., surface hopping) to account for the non-adiabatic quantum transitions. Extension of the present work along this route is under way.

ACKNOWLEDGEMENTS

[1] J. P. Gu, G. Hirsh, R. J. Buenker, I. D. Petsalakis, G. Theodorakopoulos, and M. B. Huang, Chem. Phys. Lett. **230**, 473 (1994).

[2] J. Sadlej and W. D. Edwards, Int. J. Quantum Chem. **53**, 607 (1995).

[3] S. J. Park, Y. S. Lee, and G. H. Jeung, Chem. Phys. Lett. **277**, 208 (1997).

[4] J. Ahokas, T. Kiljunen, J. Eloranta, and H. Kunttu, J. Chem. Phys. **112**, 2420 (2000).

[5] I. S. K. Kerkines and A. Mavridis, J. Chem. Phys. **116**, 9305 (2002).

[6] W. Baylis, J. Chem. Phys. **51**, 2665 (1969).

[7] J. Pascale and J. Vandeplanque, J. Chem. Phys. **60**, 2278 (1974).

[8] R. Düren and G. Moritz, J. Chem. Phys. **73**, 5155 (1980).

[9] R. Düren, E. Hasselbrink, and G. Moritz, Z. Phys. A **307**, 1 (1982).

[10] E. Czuchaj and J. Zenkiewiecz, Z. Naturforsch. A **34**, 694 (1979).

[11] E. Czuchaj, F. Rebentrost, H. Stoll, and H. Preuss, Chem. Phys. **136**, 79 (1989).

[12] M. B. El Hadj Rhouma, H. Berriche, Z. B. Lakhdar, F. Spiegelman, J. Chem. Phys. **116**, 1839 (2002).

[13] V. V. Meshkov, E. A. Pazyuk, A. Zaitsevskii, A. V. Stolyarov, R. Brühl, and D. Zimmermann, J. Chem. Phys. **123**, 204307 (2005).

[14] L. A. Blank, G. S. Kedziora, and D. E. Weeks, Proc. SPIE 7581, High Energy / Average Power Lasers and Intense Beam Applications IV, 75810I(); doi: 10.1117/12.845215 (2010).

[15] F. B. Salem, M. B. El Hadj Rhouma, N. Khelifi, J. Clust. Sci. **23**, 115 (2012).

[16] E. Jacquet, D. Zanuttini, J. Douady, E. Giglio, and B. Gervais, J. Chem. Phys. **135**, 174503 (2011).

[17] J. Vigue, Phys. Rev. A **52**, 3973 (1995).

[18] A. Martínez-Mesa, L. Uranga-Piña, G. Rojas-Lorenzo, J. Rubayo-Soneira, Chem. Phys. Lett. **426**, 318 (2006).

[19] A. Martínez-Mesa, L. Uranga-Piña, Rev. Cub. Fis. **29**, 72 (2012).

[20] M. L. Klein, V. A. Venables (Eds.), Rare Gas Solids (Academic Press, New York, 1977).

[21] N. W. Ashcroft, N. D. Mermin, Solid State Physics, (Saunders, Philadelphia, 1976).

[22] L. C. Balling and J. J. Wright, J. Chem. Phys. **79**, 2941 (1983).

[23] J. A. Boatz and M. E. Fajardo, J. Chem. Phys. **101**, 3472 (1994).

[24] L. Uranga-Piña, A. Martínez-Mesa, J. Rubayo-Soneira, G. Rojas-Lorenzo, Chem. Phys. Lett. **429**, 450 (2006).

[25] G. Rojas-Lorenzo, J. Rubayo-Soneira, S. Fernandez Alberti, and M. Chergui, J. Phys. Chem. A **107**, 8225 (2003).

[26] R. A. Corbin and M. E. Fajardo, J. Chem. Phys. **101**, 2678 (1994).

18